THEORETICAL AND APPLIED MECHANICS
Volume 51 (2024) Issue 1, 27–38 DOI: https://doi.org/10.2298/TAM230523002M

INVESTIGATING INTERFACIAL CRACKS IN BI-MATERIALS THROUGH A 4-POINT BENDING MODEL ANALYSIS

Abdeljelil Mankour and Bachir B. Belabbes

Abstract. This study focuses on examining the failure behavior of interfacial cracks in bimaterial structures. Bimaterials present a unique challenge due to their composition, consisting of two materials that can be homogeneous and isotropic, with a specific emphasis on the ceramics/metal combination. The disparity in elastic and physical properties between these materials leads to stress singularities and embrittlement of the interface. In order to investigate the behavior of an interfacial crack without propagating into the individual materials, numerical simulations of a 4-point bending model were conducted. The stress intensity factors were computed at the crack tip to determine the energy release rate, which is a crucial parameter in evaluating interfacial crack behavior. The energy release rate, along with the mixed mode angle (G, ψ), provides insights into the crack's response. The findings demonstrate that an increase in the thickness ratio (H_1/H_2) of the assembled materials, as well as a reduction in the Young's modulus ratio (E_1/E_2), result in higher energy release rates for interfacial cracks in bimaterials. This indicates that the properties of the assembled materials play a significant role in determining the dominant mode of crack propagation tendency.

1. Introduction

Interfacial cracks play a significant role in fracture mechanics and are characterized as cracks occurring along the interface between two distinct materials [1]. In various industries including aerospace, mechanical, biomedical and automotive, where multi-layer materials such as composite laminates and adhesive structures are extensively used, the propagation of interface cracks leading to delamination failure is a common occurrence [2–4]. In addition, modern devices exhibit intricate architectures, employ diverse materials, and incorporate small-scale features [5, 6]. Within these devices, various processes such as material deposition, temperature fluctuations, and electro-migration give rise to stresses [7, 8]. The presence of

2020 *Mathematics Subject Classification:* 74B05; 74E30; 74Rxx; 74S05.
Key words and phrases: bimaterials, interfacial crack, energy release rate, mixed mode, finite element method.

stresses can lead to the separation of dissimilar materials, which represents a predominant failure mode for such devices. Hasan et al. conducted a study examining the influence of electromigration and delamination on the failure modes affecting the output power of photovoltaic modules. The findings revealed a decrease in the modules' overall lifetime due to these factors [9]. Wei et al. conducted a study on electromigration-induced extrusion failures in Cu/low-k interconnects, where the propagation of cracks originates from voids at the interface [10]. When dealing with metal/ceramic joints, a critical aspect of consideration is the energy release rate associated with interface fracture. This is primarily due to the fact that the interface typically represents the weakest region in such combined materials. Notably, the impact of interface strength, material properties, and specimen geometry on the energy release rate holds significant importance [11, 12].

Linear Elastic Fracture Mechanics (LEFM) is applied in this work to examine a bimaterial configuration that includes an initial crack. LEFM is employed for its simplicity, predictive capabilities, and widespread acceptance in assessing the behavior of interfacial cracks in bimaterials. A key concept in LEFM is the stress intensity factor (K), which quantifies the intensity of the stress field near the crack tip. It is a measure of the tendency for crack propagation and crucial for predicting crack growth. LEFM assumes that the plastic zone near the crack tip is negligible compared to the overall size of the structure. This assumption facilitates the use of linear elastic principles. Thus, this theory describes the particularity of the stress state induced by a crack appearing at the interface between two dissimilar materials. The presence of cracks in brittle materials indicates a predominant influence on mode I. On the other hand, in the case of bimaterials, the interfacial crack tends to evolve towards a mixed mode. This progression is notably governed by the difference in elastic properties between the materials that are jointly bonded. This mode of crack is identified as mode I (opening) and mode II (shearing). Recent studies indicate that the rupture process is determined by the proportion of displacement in shearing [13]. On one hand, it acts on the crack energy, and on the other hand, on the direction of crack propagation [14].

When both materials are considered as elastic, homogeneous and isotropic with shear modules μ_1 and μ_2, Poisson's ratios ν_1 and ν_2, respectively, the stress field depends on the two Dundurs' elastic mismatch parameters [15], (figure 1). Dundurs observed that the solutions to plane problems of elasticity for bimaterials depend on these two non-dimensional combinations of the elastic modules α, β defined by the equations 1 and 2:

$$\alpha = \frac{\mu_1(\chi_2+1) - \mu_2(\chi_1+1)}{\mu_1(\chi_2+1) + \mu_2(\chi_1+1)} = \frac{E_1' - E_2'}{E_1' + E_2'} \tag{1.1}$$

$$\beta = \frac{\mu_1(\chi_2+1) - \mu_2(\chi_1+1)}{\mu_1(\chi_2+1) + \mu_2(\chi_1+1)} = \frac{E_1' - E_2'}{E_1' + E_2'} \tag{1.2}$$

$$\text{with: } \left[\chi_j = \begin{cases} \dfrac{3-\nu_j}{1+\nu_j} & \text{in plane stress} \\ \chi_j = 3 - 4\nu_j & \text{in plane strain} \end{cases}\right] \left[E_j' = \begin{cases} E_j & \text{in plane stress} \\ \dfrac{E_j}{1-\nu_j^2} & \text{in plane strain} \end{cases}\right] \tag{1.3}$$

Where μ, ν, and a are the shear modulus, Poisson's ratio, and crack length, respectively, and subscripts 1 and 2 refer to the materials above and below the interface, respectively. E_1 and E_2 are the Young's moduli of the two materials.

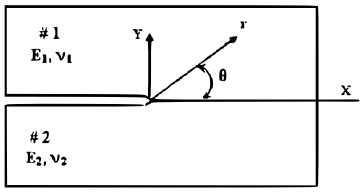

FIGURE 1. Interfacial crack

Figure 2 illustrates a parallelogram featuring different bimaterial couples [16].

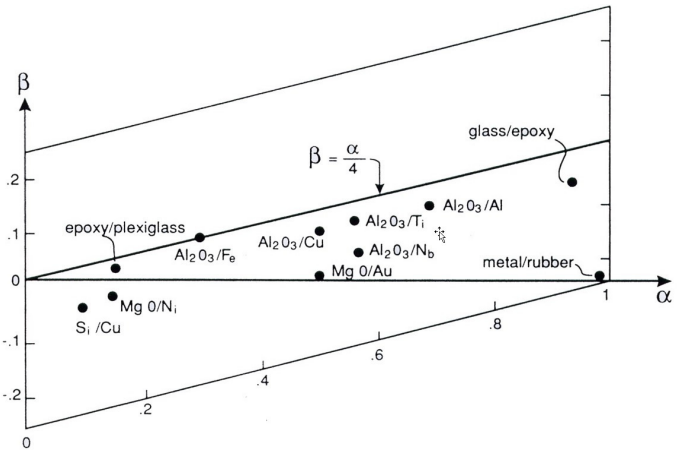

FIGURE 2. Values of Dundur's parameters of some bimaterial couples

In the case of a homogeneous material, the two Dundurs' parameters are null ($\alpha = \beta = 0$), and for the presence of a very rigid component $\alpha = \pm 1$. When materials 1 and 2 are reversed (1 situated in $y < 0$ and 2 situated in $y > 0$); α and β change sign preserving the absolute value. In the case of a metal/ceramic combination, the values of the Dundurs' parameter ($\alpha = 0.8 - 0.9$) are important [16, 17].

The stress field for an interfacial crack is characterized by a mixed mode. Such a field can extend to the forefront of the crack interface between two dissimilar materials, leading to a complex stress intensity factor:

$$K = K_{\mathrm{I}} + iK_{\mathrm{II}} \tag{1.4}$$

Where: K_{I} and K_{II} represent the real and imaginary parts of the complex stress intensity factor, respectively.

The factors K_{I} and K_{II} cannot be directly interpreted as the mode I or mode II stress intensity factors. So, in order to introduce a characteristic quantity which represents mode I and mode II, one may define the mixed mode ratio ψ as the angle represented by ψ. The term ψ [18] measures the proportion of solicitations in opening and in shearing modes at an interfacial crack tip.

$$\psi = \arctan\left(\frac{K_{\mathrm{II}}}{K_{\mathrm{I}}}\right) \tag{1.5}$$

The values of ψ are ranging between $-\frac{1}{2}$ and $\frac{1}{2}$; for ψ equal to $-\frac{1}{2}$ and $\frac{1}{2}$, the crack propagation is dominated by a pure mode II (shearing mode). For $\psi = 0$, the crack propagates in pure mode I (opening mode). For $-\frac{1}{2} < \psi < 0$ and $0 < \psi < \frac{1}{2}$, the propagation process is conducted by a mixed mode.

The energy release rate, G, is commonly employed in modeling the fracture process due to its proportional relationship with the sum of squared values of the generalized stress intensity factor [18].

$$G = \frac{\frac{1}{E_1'} + \frac{1}{E_2'}}{2\cosh^2(\pi\varepsilon)}(K_{\mathrm{I}}^2 + K_{\mathrm{II}}^2) \tag{1.6}$$

The bimaterial constant ε is responsible for the main differences of the linear elasticity solution for interfacial cracks in comparison to cracks in a homogeneous material, where ε is defined by:

$$\varepsilon = \frac{1}{2\pi}\ln\left(\frac{1-\beta}{1+\beta}\right) \tag{1.7}$$

The aim of this survey is to simulate the interfacial cracks in bimaterials of the type ceramic/metal using 4-point bending analysis and subjected to identical loading conditions. A 2-D finite element method is used to analyze the behavior of an interfacial crack by the computation of SIF K_{I} and K_{II}, the calculation of normalized energy release rate G/G_0, and the mixed mode angle ψ for different metal thicknesses and mechanical properties of assembled materials using equations (1.5) and (1.6). In all analyses, the interfacial fracture energy release rate G is normalized by:

$$G_0 = \frac{\sigma^2\pi a}{E_2} \tag{1.8}$$

2. Finite Elements Analysis

2.1. Geometrical model and mesh. In this analysis, we employed a 4-point bending test to simulate an interfacial crack scenario. The focus was on investigating cracked bimaterials, composed of two distinct materials with different mechanical properties (ceramics E_2, ν_2 and metal E_1, ν_1) (Figure 3). The bimaterial beam had a length (L) equal to twice its width (W), where W corresponded to the sum of the metal (H_1) and ceramic (H_2) thicknesses. A concentrated loading of F was applied to the beam (Figure 3). To simplify the modeling process and account for geometric and loading symmetry, only half of the structure was modeled (see Figure 4).

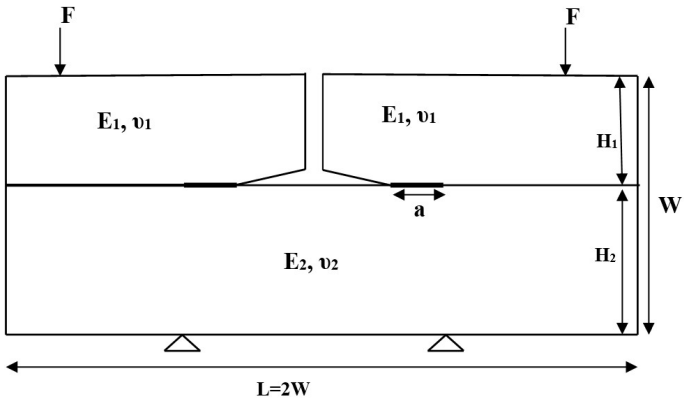

FIGURE 3. Geometrical model of 4-point bending

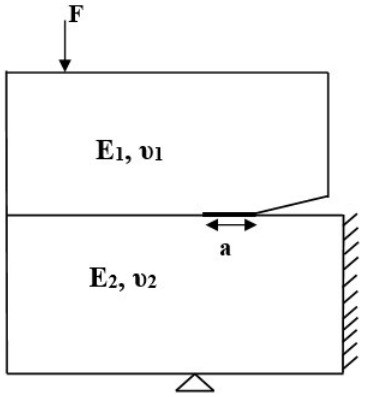

FIGURE 4. Half model due to symmetry

For this analysis, a two-dimensional model was constructed using eight-noded quadrilateral plane stress elements (CPS8R) (Figure 5). Mesh parameters were carefully defined to ensure appropriate element sizes in various regions, with a particular focus on refining the mesh near the crack tip (Figure 5). The finite element analysis (FEA) model was refined to ensure a precise representation of the interfacial crack behavior in the bimaterials model.

To ensure the reliability and accuracy of the results, a mesh convergence study was performed. A series of simulations with consistent boundary conditions were executed, progressively refining the mesh sizes. Convergence was considered achieved when the stability of the output results, specifically the stress intensity factors, demonstrated a difference of less than 2% between sequentially refined mesh sizes. This convergence criterion allowed for the confident determination of the optimal mesh size required to effectively capture the behavior of the system and obtain accurate results.

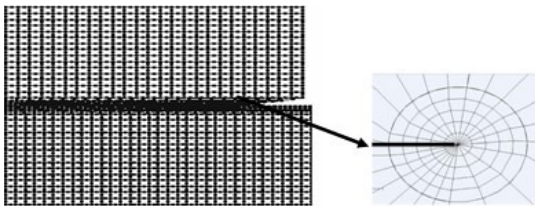

FIGURE 5. Model mesh and crack tip

One supposes state of the plane stress conditions. The relevant parameters and Young's modulus ratio values for the bimaterial combinations used in this analysis are presented in Table 1. This table provides an overview of the Dundurs' parameters and Young's modulus ratio for each bimaterial combination employed in the study.

TABLE 1. Dundurs' parameters and Young's modulus ratio of different bimaterial couples

Couples	α	β	E_1/E_2
Al_2O_3/Al	0.67	0.191	0.2
Al_2O_3/Ag	0.64	0.182	0.22
Al_2O_3/Cu	0.46	0.133	0.36
Al_2O_3/Au	0.42	0.121	0.4
Al_2O_3/Ni	0.26	0.076	0.58
Al_2O_3/ThO_3	0.05	0.015	0.89

3. Results and Discussions

In our analysis, we concentrate on a state of plane stress, confining our study to a two-dimensional analysis wherein the impact of thickness is considered negligible, and consequently, we involve the concepts from Linear Elastic Fracture Mechanics (LEFM) and examine the stress field around the crack tip. We operate under the assumption of linear elastic behavior for the bimaterial.

The obtained results are represented in Figure 6, which illustrates the variation of the standardized energy release rate G/G_0 according to the thickness ratios H_1/H_2 of the two constituting materials, for a constant crack length of $a/W = 0.04$. We notice that for all cases of the Young's modulus ratio values E_1/E_2, the energy release rate is proportional to the thickness ratio H_1/H_2. Furthermore, the interfacial fracture energy depends strongly on the thickness ratio H_1/H_2; a high metal thickness leads to a significant energy value which can lead to the junction fracture [19, 20]. Thus, the decrease of metal thickness involves a stress field reduction at the crack tip which causes a reduction in fracture energy and consequently the crack propagation. Also, ceramic materials have low toughness which can be improved by mechanisms that shield the crack tip [21–24].

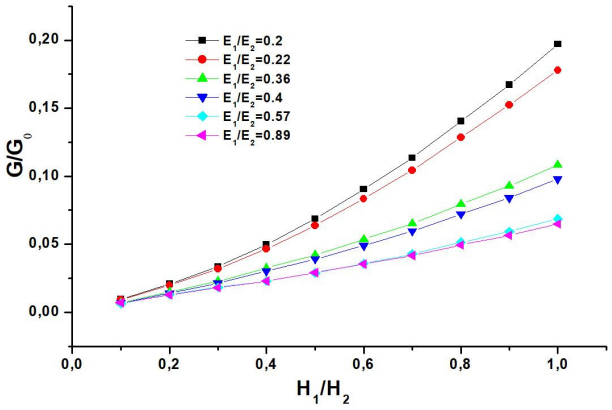

FIGURE 6. G/G_0 vs. Metal/Ceramic ratio H_1/H_2

In the case of H_1/H_2 ratio close to 1, the energy release rate decreases considerably with the increase of Young's modulus ratio E_1/E_2. This propensity is less significant when the metal thickness H_1 is thinner. As a result, the amount of energy release rate augments proportionally to the thickness ratio of assembled materials and becomes significant following the increase of metal Young's modulus; consequently, the propensity for crack propagation becomes more prominent.

To verify the accuracy of the G/G_0 values obtained, a comparison was made between the energy release rate determined through the finite element analysis and the analytically calculated normalized G/G_0 using equation 3.2. The outcomes are depicted in Figure 7. For this specific investigation, the bimaterial couple "$Al_2O_3 - Al$" was used, and a fixed interfacial crack length of $a/W = 0.04$ was employed.

$$G_{\text{numerical}} = \frac{1/E_1 + 1/E_2}{\cosh^2(\pi\varepsilon)}(K_{\text{I}}^2 + K_{\text{II}}^2) \tag{3.1}$$

$$G_{\text{analytical}} = \frac{3}{2}\left[\frac{1}{\eta_2^3} - \frac{\lambda}{\eta_1^3 + \lambda\eta_2^3 + 3\lambda\frac{\eta_1\eta_2}{\eta_1+\lambda\eta_2}}\right] \tag{3.2}$$

where $\eta_i = H_i/H$, $i = 1, 2$, and $\lambda = \frac{(1-\nu_1^2)E_2}{(1-\nu_2^2)E_1}$ for plane stresses. The results demonstrate a close resemblance between the two curves, indicating a strong agreement between the analytically calculated and the numerically obtained values of normalized energy release rate. This agreement is particularly notable when the thickness ratio (H_1/H_2) of the assembled couples is small and tends to diverge as the ratio approaches unity (i.e., when the metal and ceramic thicknesses are nearly equal). It is worth noting that the disparity between the results is approximately 10% when the thickness ratio is 1 (representing equal metal and ceramic thicknesses). To gain a better understanding of the impact of the H_1/H_2 ratio on the fracture energy at the crack tip, we conducted a reverse configuration by increasing the thickness of the ceramics while keeping the metal thickness constant. Figure 8 showcases the

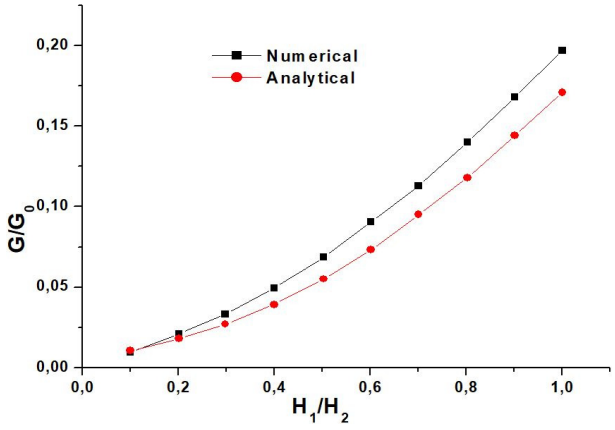

FIGURE 7. Comparison of analytical and numerical values of G/G_0 vs. H_1/H_2

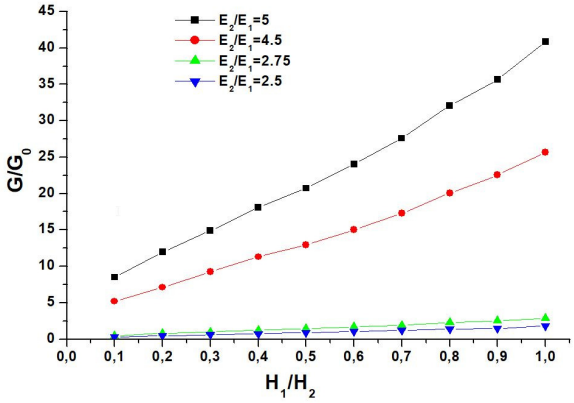

FIGURE 8. G/G_0 vs. Thickness ratios H_1/H_2 (reversed bimaterials combination)

variation of G/G_0 with respect to the thickness ratio H_1/H_2 for different reversed bimaterial couples, with a fixed interfacial crack length of $a/W = 0.04$. Thus, we notice a similar trend in the normalized energy as observed in the previous analysis for all ceramic/metal couples. Specifically, the rupture energy at the interfacial crack tip increases as Young's modulus of the assembled metal decreases. In addition, the energy release rate of reversed bimaterials is 600 times greater than the metal/ceramic ones when $H_1/H_2 = 0.1$ and decreases, reaching 200 times for $H_1/H_2 = 1$. Consequently, the energy values increase significantly when compared to the previously analyzed normalized rupture energy. In Figure 9, we present the variation of normalized energy release rate according to the Young's modulus

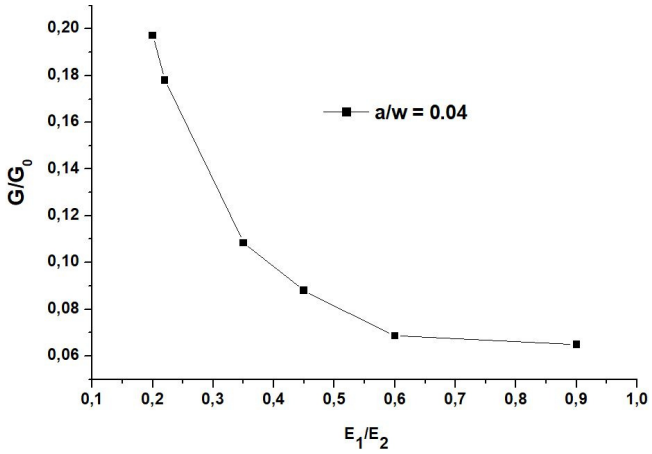

FIGURE 9. G/G_0 vs Young's modulus ratio E_1/E_2 (case $H_1/H_2 = 1$)

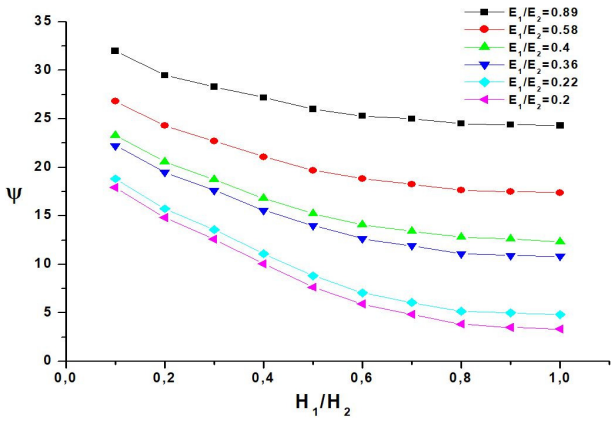

FIGURE 10. Mixed mode parameter ψ versus thickness ratio H_1/H_2

ratio of bimaterials. The fracture energy at the crack tip depends on the assembled materials. According to the findings, there is a reduction in rupture energy as the Young's modulus ratio (E_1/E_2) increases, reaching a stabilization point around $E_1/E_2 = 0.6$. We notice that the higher rigidity of the assembled metal gives significant rupture energy at the interfacial crack tip. These results confirm the previous finding. The analysis of interfacial crack allows us to evaluate the variation of the mixed mode parameter ψ according to the thickness ratio of ceramic/metal couples H_1/H_2 and a different Young's modulus ratio E_1/E_2 (see Figure 10). We notice that, for the lower Young's modulus ratios $E_1/E_2 = 0.2$, the mixed mode angle ψ is minimal and increases with the augment of E_1/E_2. Moreover, the mixed mode angle reduces by the increase of H_1/H_2 ratio. Thus, mixed mode angle ψ stabilizes

when the values of thickness ratio H_1/H_2 is greater than 0.7. Therefore, the lower ratio H_1/H_2 gives a higher mixed mode angle, where mode I dominates; and when the Young's modulus of assembled bimaterials are close, ψ decreases and tends to stabilize; thus, the shearing mode dominates in this case.

In Figure 11, we presented the variation of G/G_0 according to the mixed mode angle ψ. It is noticed that the maximum of normalized energy release rate $G/G0$ is reached when ψ is minimal, and it becomes of lower intensity for larger values of the mixed mode angle. Hence, the sliding mode dominates the stresses at the interfacial crack tip.

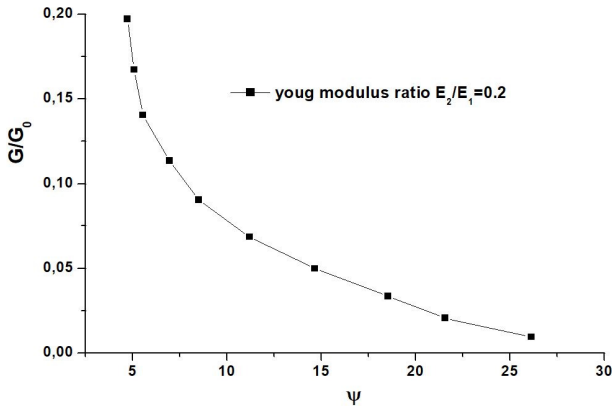

FIGURE 11. G/G_0 versus mixed mode angle ψ

4. Conclusion

This study aimed to investigate the behavior of interface cracks in bimaterials under mechanical loading using the finite element method. A thorough examination of various fracture parameters, such as the energy release rate and mixed mode angle, was conducted to assess their significance in the studied context. The findings regarding the rupture behavior of bimaterials revealed that the energy release rate increases as the thickness of the metal component increases, but decreases as the ratio of Young's modulus (E_1/E_2) increases. Thus, the fracture energy at the crack tip in the interface is influenced by the properties of the joined materials. Consequently, interfacial cracks tend to propagate under a mixed mode. However, the normalized energy release rate (G/G_0) is inversely proportional to the mixed mode angle (ψ), indicating that the normalized energy release rate decreases as the mixed mode angle increases.

References

1. J. W. Hutchinson, Z. Suo, *Mixed mode cracking in layered materials*, Adv. Appl. Mech **29** (1991), 63–191.
2. X. J. Feng, X. Q. Yan, Y. T. Wei, X. W. Du, *Analysis of extension propagation process of interface crack between belts of a radial tire using a finite element method*, Appl. Math. Model. **28**(2) (2004), 145–162.

3. A. Afshar, S. Hatefi Ardakani, S. Mohammadi, *Stable discontinuous space-time analysis of dynamic interface crack growth in orthotropic bi-materials using oscillatory crack tip enrichment functions*, Int. J. Mech. Sci. **140** (2018), 557–580.
4. M. Pant, I. V. Singh, B. K. Mishra, *Evaluation of mixed mode stress intensity factors for interface cracks using EFGM*, Appl. Math. Model **35**(07) (2011), 3443–3459.
5. M. A. Hussein., J. He, *Materials impact on interconnects process technology and reliability*, IEEE Trans. Semicond. Manufact. **18**(1) (2005), 69–85.
6. Z. Suo, *Reliability of interconnect structures*, In: W, Gerberich, W. Yang, (eds.), Interfacial and nanoscale failure, Comprehensive structural integrity **8** (2003), 265–324.
7. W. D. Nix, *Mechanical-properties of thin-films*, Metal. Trans **20**(A) (1989), 2217–2245.
8. L. B. Freund, S. Suresh, *Thin Film Materials: Stress, Defect Formation and Surface Evolution*, Cambridge, Cambridge University Press, 2002.
9. A. A. Q. Hasan, A. Ahmed Alkahtani, S. A. Shahahmadi, M. N. E. Alam, M. A. Islam, N. Amin, *Delamination-and electromigration-related failures in solar panels—a review*, Sustainability. **13** (2021), 6682.
10. F. L. Wei, C. L. Gan, T. L. Tan, S. H. R. Christine, A. P. Marathe, J. J. Vlassak, C. V. Thompson, *Electromigration-induced extrusion failures in Cu/low-k interconnects*, J. Appl. Phys. **104**(2) (2008), 023529.
11. G. Elssner, D. Korn, M. Ruhle, *The influence of interface impurities on fracture energy of UHV diffusion bonded metal-ceramic bicrystals*, Scripta Metallurgica et Materialia **31** (1994), 1037–1042.
12. F. Gaudette, S. Suresh, A. G. Evans, G. Dehm, M. Rfuhle, *The influence of chromium addition on the toughness of γ-Ni/α-Al_2O_3 interfaces*, Acta Mater. **45**(9) (1997), 3503–3513.
13. D. Katsareas, N. Anifantis, *Boundary element analysis of thermally stresses interface crack*, Eng. Fract. Mech. **50** (1995), 51–60.
14. B. Bachir Bouiadjra, M. Belhouari, M. Benguediab, B. Serier, *Numerical analysis of the behaviour of bi-material interface notch crack, contact mechanics*, Trans. on Eng. Sci. **32** (2001), 77–86.
15. J. Dundurs, *Effect of elastic constants on stress in a composite under plane deformation*, Compos. Mater. **1** (1969), 310–322.
16. T. Suga, G. Elssner, S. Schmauder, *Composite parameters and mechanical compatibility of material joint*, J. Comp. Mat. **22** (1988), 917–934.
17. C. T. Sun, C. J. Jih, *On strain energy release rates for interfacial cracks in bimaterials media*, Eng. Fract. Mech. **28**(1) (1987), 13–20.
18. J. R. Rice, *Numerical analysis for micro-vibration isolation of jointed sandwich plates with mass blocks*, J. Appl. Mech. **55** (1988), 98–103.
19. W. Mekky, P. S. Nicholson, *The fracture toughness of Ni/Al_2O_3 laminates by digital image correlation I: Experimental crack opening displacement and R-curves*, Eng. Fract. Mech. **73**(5) (2006), 571–582.
20. W. Mekky, P. S. Nicholson, *The fracture toughness of Ni/Al_2O_3 laminates by digital image correlation II: Bridging-stresses and R-curve models*, Eng. Fract. Mech. **73**(5) (2006), 583–592.
21. M. C. Shaw, D. B Marshall, M. S. Dadkhah, A. G. Evans, *Cracking and damage mechanisms in ceramic/metal multilayers*, Comput. Methods Appl. Mech. Eng. **41**(11) (1993), 3311–3322.
22. O. Sbaizero, G. Pezzotti, *Tailoring the microstructure of a metal-reinforced ceramic matrix composite*, J. Eng. Mater.Technol. **122** (2000), 363–367.
23. A. G. Evans, *Structural reliability: a processing-dependent phenomenon*, J. Am. Ceram. Soc. **65**(3) (1982), 127–137.
24. P. F. Becher, *Microstructural design of toughened ceramics*, J. Am. Ceram. Soc. **74**(2) (1991), 255–269.

ИСТРАЖИВАЊЕ ПУКОТИНА У ДВО-МАТЕРИЈАЛИМА КРОЗ АНАЛИЗУ МОДЕЛА САВИЈАЊА У 4 ТАЧКЕ

Резиме. Ово истраживање се фокусира на испитивање понашања лома међуповршинских пукотина у двоматеријалним структурама. Двоматеријали представљају јединствен изазов због свог састава, који се састоји од два материјала који могу бити хомогени и изотропни, са посебним нагласком на комбинацију керамика/метал. Диспаритет у еластичним и физичким својствима између ових материјала доводи до сингуларности напона и крхкости међуповршине. Да би се истражило понашање међуповршинске пукотине без ширења у појединачне материјале, спроведене су нумеричке симулације модела савијања у 4 тачке. Фактори интензитета напрезања су израчунати на врху прслине да би се одредила брзина ослобађања енергије, што је кључни параметар у процени понашања међуповршинских пукотина. Брзина ослобађања енергије, заједно са углом мешовитог режима (G, ψ), пружа увид у реакцију пукотине. Налази показују да повећање односа дебљине (H_1/H_2) спојених материјала, као и смањење односа Јунговог модула (E_1/E_2), резултирају већим брзинама ослобађања енергије за међуповршинске пукотине у двоматеријалима. Ово указује да својства спојених материјала играју значајну улогу у одређивању доминантног начина тенденције ширења прслине.

Satellite development center (CDS)
Oran
Algeria
m_abdeldjalil@yahoo.fr
https://orcid.org/0000-0001-6024-0944

LMPM, Department of Mechanical Engineering
University of Sidi Bel Abbes
Sidi Bel Abbes
Algeria
bachirbou@yahoo.fr

(Received 23.05.2023)
(Revised 17.01.2024)
(Available online 15.04.2024)